Dynamic Fluctuations of Semiflexible Polymers

R. Everaers*†, F. Jülicher*, A. Ajdari+, A.C. Maggs+

+ *Physico-Chimie Théorique, ESPCI, 10 rue Vauquelin, 75231 Paris Cedex 05, France.*

* *Physico-Chimie Curie, 26 rue d'Ulm, 75248 Paris Cedex 05, France.*

† *Max-Planck-Institut für Polymerforschung, Postfach 3148, D-55021 Mainz, Germany.*

(31 July 1998)

We develop a scaling theory to describe dynamic fluctuations of a semiflexible polymer and find several distinct regimes. We performed simulations to characterize the longitudinal and transverse dynamics; using ensemble averaging for a range of different degrees of coarse-graining we avoid the problems of slow equilibration often encountered in simulations. We find that the longitudinal fluctuations of a semiflexible object scales as $t^{7/8}$. These fluctuations are correlated over a length which varies as $t^{1/8}$. Our results are pertinent to the interpretation of high frequency microrheology experiments in actin solutions.

Experiments on actin filaments have awakened interest in the dynamics of semiflexible polymers. Although the collective behavior in the semidilute regime has attracted much attention [1], the single filament problem displays surprisingly rich dynamic features absent in the case of "flexible" polymers. This is a consequence of the highly anisotropic nature of the semiflexible polymer. The static anisotropy is characterized by the exponent for the growth of transverse fluctuations, $r_\perp$ as a function of the filament length, $L < \kappa$ [2], $r_\perp^2 \sim L^3/\kappa$ where κ is the persistence length of the filament. The dynamics is commonly described by a Langevin equation for the transverse fluctuations [3],

$$\frac{\partial r_\perp}{\partial t} = -\kappa \frac{\partial^4 r_\perp}{\partial s^4} + f_\perp(s,t) \tag{1}$$

Here, $f_\perp$ denotes a transverse stochastic force per unit length applied to the filament, s is a curvilinear coordinate and hydrodynamic interactions are neglected on the ground that they only induce logarithmic corrections. After time t, the filament is equilibrated over a length $l_1(t) \sim (\kappa t)^{1/4}$. This results in a scaling of the transverse dynamics first measured in dynamic light scattering [4], where it is seen that the transverse motion of a monomer on a filament varies as [6]

$$\langle \delta r_\perp(t)^2 \rangle \sim l_1(t)^3/\kappa \sim t^{3/4}/\kappa^{1/4} \tag{2}$$

The longitudinal fluctuations of a filament are even more subtle. We need to impose strict incompressibility on the filament, which is violated in the simplest linearized equations such as (1). This is a long standing and delicate problem in the description of worm like polymers [5]. Recently scaling in $t^{3/4}$ has been predicted [7,8] for the longitudinal fluctuations of a filament, with however an amplitude smaller by a factor L/κ than in (2); we can also find this result with a simple scaling argument: Due to the local conservation of filament length the transverse fluctuations of a segment of length l result in parallel fluctuations of $\delta r_l \simeq \frac{1}{2}\int_0^l ds(\partial r_\perp/ds)^2$ comparable to $\langle \delta r_l^2 \rangle \sim l^4/\kappa^2$. Each section of length $l_1(t)$ of the filament is independent so that we can add the fluctuations of $m = L/l_1(t)$ segments giving the motion of the end

$$\langle \delta r_\parallel(t)^2 \rangle \sim m\, \delta r_l^2 = (L/l_1)(l_1^4/\kappa^2) = Lt^{3/4}/\kappa^{5/4} \tag{3}$$

While applicable to the case of a filament in a macroscopic shear field [8] this result is problematic for local probes of the dynamics. In particular the divergence of the fluctuations with the filament length must surely break down at some point. A similar problem exists in the athermal dynamics of semiflexible filaments [9,10] where the longitudinal friction of the filament modifies the dynamics. It is the purpose of this letter to explore the importance of longitudinal dissipation and the incompressibility constraint in the dynamics of the fully thermalised chain.

In the derivation leading to (3), longitudinal friction is absent and all the different segments of length $l_1(t)$ contribute by their longitudinal fluctuations to the motion of the end. However, the shortening (or extension) of a segment also requires the longitudinal motion of its neighbors. As a consequence, longitudinal friction limits the number of segments which can contribute within a finite time. Typically this limitation should not be significant if the longitudinal diffusion of the whole polymer (diffusing as $r^2 = t/L$) is so fast that there is no hindrance to the cumulation of fluctuations. This introduces a criterion for the validity of Eq. (3): $Lt^{3/4}/\kappa^{5/4} < t/L$ or $L < l_2(t) = t^{1/8}\kappa^{5/8}$. For longer filaments only a section of length $l_2(t)$ can contribute to the fluctuation of the end point. This limitation thus amounts in substituting l_2 for L in (3):

$$\langle \delta r_\parallel(t)^2 \rangle \sim t^{7/8}/\kappa^{5/8} \tag{4}$$

A similar result can be found from an analysis of the linear response of a filament to a weak constant longitudinal force $f_\parallel$ using the fluctuation dissipation theorem [11]. Equation (3) predicts that in the presence of a force the end drifts as $\delta r_\parallel(t) \sim f_\parallel L t^{3/4}/\kappa^{5/4}$. However we cannot set the whole filament into motion at once: the typical velocity scales as $v_\parallel \sim \delta r_\parallel/t \sim f_\parallel L/\kappa^{5/4}t^{1/4}$, and the total drag $Lv_\parallel$ can not be larger than the applied force. This requirement again reads $L < l_2(t)$. For a long filament the tension propagates a distance $l_2(t)$. The corresponding section along which tension has propagated is set into motion at a velocity of the order of $v_\parallel \approx f_\parallel/l_2$ and the end drifts a distance $\delta r_\parallel(t) \sim f_\parallel t^{7/8}/\kappa^{5/8}$, in agreement with (4).

Thus a surprising conclusion is that there are *two dynamic length scales* which play important roles in the dynamics of filaments. Our main result is thus that the dynamics obey a pair of scaling relations with different scaling arguments. In particular, the fluctuations of the end of a filament are expected to follow:

$$\langle \delta r_\parallel(t)^2 \rangle = \frac{t^{7/8}}{\kappa^{5/8}} \mathcal{Q}\left(\frac{t^{1/8}\kappa^{5/8}}{L}\right) \tag{5}$$

$$\langle \delta r_\perp(t)^2 \rangle = \frac{t^{3/4}}{\kappa^{1/4}} \mathcal{W}\left(\frac{t^{1/4}\kappa^{1/4}}{L}\right) \tag{6}$$

In the rest of this paper we present computer simulations of a model filament in order to check these scaling arguments.

We have performed simulations of a semiflexible polymer in two dimensions imposing a constraint on the contour length using the technique described in [12]. The polymer is discretized with sequence of beads with positions $\vec{r}_i$, $i \in 0 \ldots n$, with fixed distance

$b = |\vec{r}_i - \vec{r}_{i-1}|$ and normalized bond vectors $\vec{d}_i = (\vec{r}_i - \vec{r}_{i-1})/b$. The angles θ_i characterizing the bond directions are coupled by simple angular springs:

$$E = \frac{1}{2}\sum_{i=1}^{n-1}\frac{\kappa}{b}(\theta_i - \theta_{i+1})^2 \tag{7}$$

The beads move against an isotropic friction $-b\partial\vec{r}_i/\partial t$ under the influence of the forces due to the angular springs, $-\partial E/\partial\vec{r}_i$ and stochastic forces $\vec{F}_i^{\mathrm{ra}}$:

$$b\frac{\partial\vec{r}_i}{\partial t} = -\frac{\partial E}{\partial\vec{r}_i} + \vec{F}_i^{\mathrm{ra}} + T_{i+1}\vec{d}_{i+1} - T_i\vec{d}_i \tag{8}$$

The tensions T_i play the role of Lagrange multipliers whose values are calculated at each time step from the condition that the bond lengths are equal to b.

The shortest characteristic time of the model is approximately $\tau(b) = b^4/\kappa$, while the relaxation time of a chain of $n = L/b$ segments varies as $\tau_n \sim n^4\tau(b)$. The total simulation time needed to equilibrate a chain is proportional to n^5. The equilibration of long chains becomes quickly impossible; previous studies have been limited to chains which are too short to study detailed features of the dynamics.

We get around the problem of generating independent configurations by simulating long chains for a time *far* shorter than the equilibration time but then performing ensemble averages over many short runs. These simulations are useful because we can easily prepare *fully equilibrated* initial conformations for the energy eq. (7) by drawing bond angles $\delta\theta = \theta_i - \theta_{i-1}$ randomly from a Gaussian distribution $P(\delta\theta) \sim \exp\left(-\frac{\kappa}{2b}\delta\theta^2\right)$. The choice of the segmentation then determines a window of accessible time scales. The elementary time step of the integrater is $10^{-2}\tau(b)$; times shorter than $\tau(b)$ are affected by discretization errors. We generated data for times up to $10^3\tau(b)$ with a computational effort proportional to only n^1. We chose a sequence of segmentations $b_j = 2^{-j}\kappa$ and studied chains of length $\kappa/8, \kappa/4, \kappa/2, \kappa$ with the number of segments varying between $n = 8$ and $n = 1024$. The overlap between adjacent time windows ($\tau_n = 2^4\tau_{n/2}$) provides a convenient check on the coarse graining procedure and the scaling of the parameters.

We note that imposing a constraint on the bond lengths provides access to longer simulation times than simulations done with stiff longitudinal springs; we do not need to simulate the corresponding fast but uninteresting modes which limit the integration step in any explicit integration scheme. There are nevertheless complications: An extended discussion can be found in [12]. In particular, the act of passing from elastic springs to incompressible bonds changes the configuration space for the problem from Euclidean to Riemannian and the distribution function changes from $\exp(-E)$ to $\sqrt{\Delta_n}\exp(-E)$. Δ_n is the determinant of the Jacobian describing the transformation from Cartesian to bond angle coordinates which can be calculated from a transfer matrix

$$\begin{pmatrix}\Delta_{i+1}\\ \Delta_i\end{pmatrix} = \begin{pmatrix}2 & -\cos^2(\theta_i - \theta_{i+1})\\ 1 & 0\end{pmatrix}\begin{pmatrix}\Delta_i\\ \Delta_{i-1}\end{pmatrix}$$

starting from the initial vector $(2, 1)$. To recover the distribution function $\exp(-E)$ for stiff springs from a simulation of a rigid rod model, it is necessary to add a pseudo potential [13],

FIG. 1. Cloud of endpoints generated by simulating $N = 100$ realizations of the dynamics starting from the illustrated initial condition. The moments of this cloud are used to extract the longitudinal and transverse dynamical. We see that transverse fluctuations are larger in amplitude than the longitudinal fluctuations and are thus characterized by a larger moment.

$-\frac{1}{2}\log(\Delta_n)$ to E and include the corresponding forces in (8). In the simulations described in this paper a proper calculation of these forces is essential to ensure that we start our short runs from initial conformations which are properly equilibrated.

The objective of our simulations is the characterization of the transverse and longitudinal motion of the chain ends. For this purpose we perform N simulations (typically $N = 1000$) starting from an identical pre-equilibrated conformation; each simulation uses an independent series of random forces. We then record the N coordinates of one end of the chain as a function of time which form an evolving two dimensional cloud in the (x, y) plane. The cloud of points, Fig. 1, can be characterized by two important invariants, its two moments of inertia $\lambda_1(t)$ and $\lambda_2(t)$ $(\lambda_1 > \lambda_2)$. The evolution of the $\lambda_i(t)$ characterizes the transverse and longitudinal movement of the end of the chain (indeed $\lambda_i \sim \delta r^2$). We prepare a total of M random realizations (typically $M = 100$) of the initial chain over which we can calculate average properties of the cloud performing a total of $MN = 10^5$ simulations, Fig 2. For short times the evolution of the cloud is very anisotropic, and the transverse dynamics corresponds to the larger moment $\lambda_1(t)$ which scales according to eq. (2). The smaller moment $\lambda_2(t)$ characterizes the parallel motions of the filament and for short times varies in agreement with eq. (4). For long times with $l_2 > L$, a crossover to free diffusion of the whole filament occurs.

In order to understand better the relative importance of internal modes and center of mass diffusion in contributing to Eq. (5) we examined the joint motion of the two end-points of a chain. In a series of M simulations one generates a distribution of points in four dimensions (4D): $\{(x_1, x_2, y_1, y_2)\}$. The cumulants of this distribution can be used via the fluctuation dissipation theorem to calculate the response of the chain ends to arbitrary combinations of end forces [11]. We are interested in the evolution of the four moments

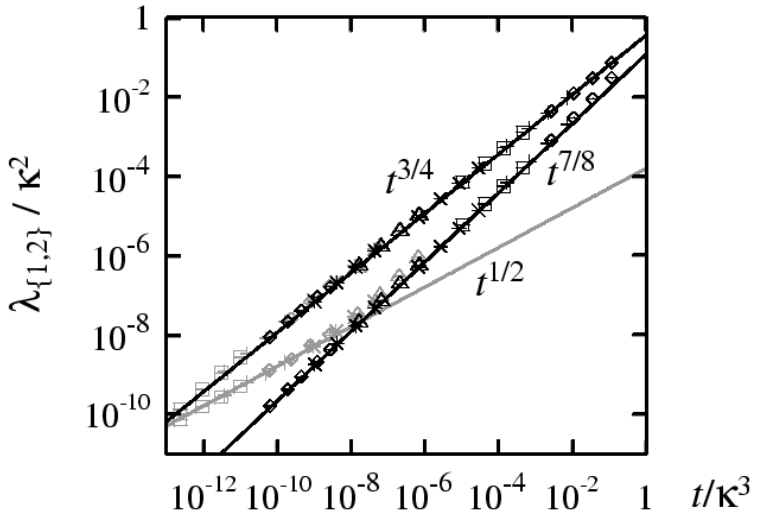

FIG. 2. Amplitude of fluctuation as a function of time for an incompressible filament (black symbols, $L = \kappa$) and a compressible filament (grey symbols, $L = \kappa/4$, modulus $K = 10^7\kappa^{-1}$) determined from the moments $\lambda_1(t)$, $\lambda_2(t)$ of the 2D clouds. The longitudinal mode scales as $\lambda_2(t) = \langle \delta r_\parallel^2 \rangle \sim t^{7/8}$, the transverse modes obey $\lambda_1(t) = \langle \delta r_\perp^2 \rangle \sim t^{3/4}$. For a compressible filament, a Rouse-like scaling $\lambda_2(t) = \langle \delta r_\parallel^2 \rangle \sim t^{1/2}$ is found for very short times. The different symbols correspond to different levels of coarse-graining.

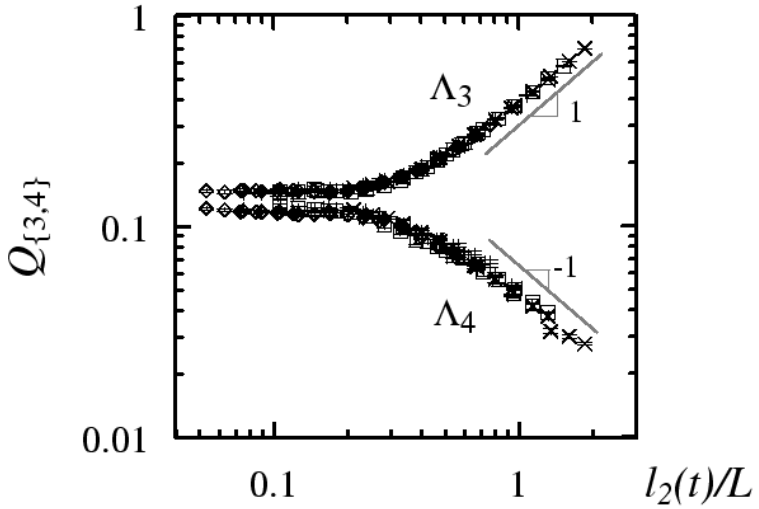

FIG. 3. Scaling behavior of the two smallest moments $\Lambda_{3,4}$ of the 4D clouds. Plotted is $\mathcal{Q}_{\{3,4\}} = \Lambda_{\{3,4\}}\kappa^{5/8}t^{-7/8}$ as a function of the tension propagation length $l_2(t) = t^{1/8}\kappa^{5/8}$ for $L = \kappa$ ($\diamond$), $\kappa/2$ ($+$), $\kappa/4$ ($\square$), $\kappa/8$ ($\times$). The plot demonstrates that the longitudinal fluctuations follow the scaling form of Eq. (5).

$\{\Lambda_1 > \Lambda_2 > \Lambda_3 > \Lambda_4\}$ of the 4D cloud which characterize the dynamics of the whole chain.

Our picture of the propagation of tension fluctuations as introduced above suggests the following scenario: As long as $l_2 < L$, the movement of the ends are uncorrelated. The 4D distribution factorises and reduces to a product of the 2D case discussed above, [15]: the two (degenerate) smaller moments $\Lambda_3 = \Lambda_4 \simeq \lambda_2$ scale as $t^{7/8}/\kappa^{5/8}$ and the two larger moments $\Lambda_1 = \Lambda_2 \simeq \lambda_1$ scale as $t^{3/4}/\kappa^{1/4}$. For longer times $l_2(t) > L$ the two ends see each other as tension propagates along the filament. This lifts the degeneracy between the two smaller moments, with Λ_4 now characterizing the end to end fluctuations so that according to (3) $\Lambda_4 \sim Lt^{3/4}/\kappa^{5/4}$, and Λ_3 characterizing the longitudinal free diffusion of the chain, $\Lambda_3 \sim t/L$. Figure 3 shows the moments Λ_3 and Λ_4 plotted normalized by $t^{7/8}/\kappa^{5/8}$ as functions of $t^{1/8}\kappa^{5/8}/L$, so that they clearly follow the scaling form Eq. (5).

Real filaments have a longitudinal compressibility. In order to study the effect and to compare different methods of modeling the dynamics we have repeated some of our simulations using harmonic potentials $E_b = \sum_{i=1}^{n} K(|\vec{r}_i - \vec{r}_{i-1}| - b)^2/2b$ representing elastic bonds with a large but finite modulus K. These simulations require an elementary time step of $10^{-2}\frac{\kappa}{Kb^2}\,\tau(b)$ are performed without the pseudo potential. The internal longitudinal dynamics are over-damped and Rouse-like ($\partial_t r_\parallel \simeq K\partial_s^2 r_\parallel$), giving fluctuations which scale as $\delta r_\parallel^2 \sim (t/K)^{1/2}$; the tension is correlated over a distance $l_3(t) \sim (tK)^{1/2}$. Compressibility thus introduces a third dynamic length l_3 in competition with those already presented. For very short times $t < \kappa^{5/3}/K^{4/3}$ the compression modes dominate over the longitudinal modes

discussed in the first part of the article as shown in Fig 2. For longer times a cross-over to the dynamic behavior of the constrained chain occurs. If we assume actin filaments to be uniform rods of Young's modulus E and radius a, $\kappa \sim Ea^4$ [23] while $K \sim Ea^2$. We expect the crossover to occur for $t \sim a^{8/3}\kappa^{1/3}$ and at a length $(a/\kappa)^{1/3}\kappa$. For actin we estimate $t^{-1} \simeq 1$ MHz, indicating that on time scales larger than 10^{-6}s the exponent 7/8 should be observable for filaments longer than 0.1κ.

We have presented results in two dimensions where bending and torsion are decoupled. In three dimensions we expect the coupling between these modes produces an even richer behavior [16]. In the case of actin, a filament of length $L = \kappa$ has a torsional mode with relaxation time $\simeq 1ms$ [17] again relaxing with a diffusive, Rouse like mode together with a new competing length scale. This introduces more features which we consider in a future publication.

Can longitudinal fluctuations of semiflexible filaments be studied experimentally? Following the motion of the end of a single filament in optical microscopy may be feasible but could prove somewhat tricky. Some form of scattering experiments sensitive to the longitudinal motions would be preferable. Normal dynamic light scattering measurements are not sensitive to longitudinal motions, however one might have some hope of introducing optical inhomogeneity [18] in actin filaments by marking with a low concentration of dye. Alternatively one might hope to immuno-attach nanometric gold beads to an actin filament and follow their movement with either video or light scattering techniques.

Several of experimental groups have studied the high frequency fluctuations [19–22] of actin solutions with beads between 0.5μm and 5μm in radius. The results have been interpreted using a theory for the macroscopic modulus of a solution of semiflexible objects starting from eq. (3). We see here that no physical cut off is needed to explain the data, longitudinal friction leads to a dynamic length scale $l_2(t)$ which cuts off the divergence with L. The beads in these experiments are sufficiently small that they should sample the point response of the chain rather than being sources of uniform shear. We have seen that the response function of a single chain has a rich scaling behavior; any experiment will sample a mixture of $\delta r^2 \sim t^1$, $t^{3/4}$, $t^{1/2}$ and $t^{7/8}$ due to the averaging over filament lengths and modes. Indeed the data when examined carefully show some curvature when plotted on a logarithmic scale. However, for dense solutions multi-chain hydrodynamic interactions are surely important, we do not have a detailed understanding of this regime.

Eventually tension propagation may be an issue in the understanding of experiments analyzing motor-filament systems, as it may e.g. control the response of a filament to the "kicks" of a collection of motors. In particular the propagation of the tension in $t^{1/8}$ will lead to an effective low frequency filter due to propagation delays.

The data in this article correspond to approximately 3×10^6 independent simulations each lasting an average of 2 seconds, using 3 months of CPU time on a UltraSparc workstation. We would like to thank Paul Chaikin, Fred Gittes, Fred Mackintosh and Jacques Prost for discussions on this work.

[1] J. Käs, H. Strey, J.X. Tang, D. Finger, E. Ezzell, E. Sackmann, P.A. Janmey, *Biophys J.*, **70**, 609-625 (1996).
[2] T. Odjik *Macromolecules* **16** , 1340, (1983).
[3] We use units for which $k_BT = 1$ as well as $\eta = 1$, where η is the friction coefficient of the filament per unit length. In these units time is a volume. For actin, 1 second $\approx 1\mu\mathrm{m}^3$.
[4] C. F. Schmidt, M. Bärmann, G. Isenberg, E. Sackmann, *Macromolecules*, **22**, 3638-3649 (1989).
[5] Harris, J. Hearst, *J. Chem. Phys.*, **44**, 2595 (1966).
[6] E. Farge, A. C. Maggs, *Macromolecules*, **26**, 5041-5044, (1993).
[7] F. Gittes and F. Mackintosh, Phys. Rev. E (in press).
[8] D. Morse, preprint.
[9] U. Seifert W. Wintz, P. Nelson, *Phys. Rev. Lett.*, **27**, 5389-5392 (1996).
[10] A. Ajdari, F. Jülicher, A.C. Maggs, *J. Phys. I*, **47**, 1823-826, (1997).
[11] D. Forster, *Hydrodynamic fluctuations, broken symmetry, and correlation functions*, (Addison-Wesley, 1983)
[12] E.J. Hinch, *J. Fluid Mech.*, **271** 219-234 (1994); P.S. Grassia, E.J. Hinch and L.C. Nitsche, *J. Fluid Mech.*, **282**, 373-403, (1995); P.S. Grassia and E.J. Hinch, *J. Fluid Mech.*, **308**, 255-288 (1996).
[13] M. Fixman, *J. Chem Phys*, **69**, 1527-1537 (1978).
[14] We can estimate the range of the fictive forces generated by the Jacobian by calculating the two eigenvalues μ_1, μ_2 of the averaged matrix. This range is expected to be comparable to $1/\log(\mu_2/\mu_1)$. When the polymer is flexible the interaction range is almost nearest neighbor generating an entropic comparable to k_BT. For semiflexible filaments $\mu_1/\mu_2 \to 1$ and the interaction becomes non-local with range $\sqrt{\kappa b}$.
[15] The short time difference between Λ_3 and Λ_4 in Fig. 3 is due to fluctuations of order of $1/N^{1/2}$.
[16] R. Goldstein, T.R. Powers, C.H. Wiggins, *Phys. Rev. Lett.*, **80**, 5232-5235 (1998).
[17] M.D. Barkley, B.H Zimm, *J. Chem. Phys.*, **70**, 2991-3007 (1979).
[18] We thank Paul Chaikin for discussions on this point.
[19] B. Schnurr, F. Gittes, F.C. MacKintosh, and C.F. Schmidt, *Macromolecules*, **30**, 7781-7792, (1997).
[20] T. Mason, A. Palmer, K. Rufener, D. Wirtz, Preprint.
[21] T. Gissler and D.A. Weitz, preprint.
[22] F. Amblard, A. C. Maggs , B. Yurke, A. Pargellis and S. Leibler, *Phys. Rev. Lett.*, **77**, 4470, (1996)
[23] F. Gittes, B. Mickey, J. Nettleton, J. Howard, *J. Cell Biol.*, **120**, 923-934 (1993).